Journal of Organometallic Chemistry 876 (2018) 35–42

Contents lists available at ScienceDirect

Journal of Organometallic Chemistry

journal homepage: www.elsevier.com/locate/jorganchem

Photoluminescence and electroluminescence of four orange-red and red organic iridium(III) complexes

Ning Su [a], You-Xuan Zheng [a, b, *]

[a] State Key Laboratory of Coordination Chemistry, Collaborative Innovation Center of Advanced Microstructures, Jiangsu Key Laboratory of Advanced Organic Materials, Nanjing National Laboratory of Microstructures, School of Chemistry and Chemical Engineering, Nanjing University, Nanjing, 210093, PR China

[b] Shenzhen Research Institute of Nanjing University, Shenzhen, 518057, PR China

ARTICLE INFO

Article history:
Received 28 May 2018
Received in revised form
29 August 2018
Accepted 17 September 2018
Available online 19 September 2018

Keywords:
Organic light-emitting diodes
Iridium(III) complex
Orange-red
Red
1-(4- (trifluoromethyl)phenyl)isoquinoline
1-(4-(trifluoromethyl)phenyl)quinazoline

ABSTRACT

Using 1-(4-(trifluoromethyl)phenyl)isoquinoline (tfmpiq) and 4-(4-(trifluoromethyl)phenyl) quinazoline (tfmpqz) as the main ligands and pyrazole pyridine derivatives (mepzpy: 2-(3-methyl-1*H*-pyrazol-5-yl) pyridine, cf3pzpy: 2-(3-(trifluoromethyl)-1*H*-pyrazol-5-yl)pyridine) as the ancillary ligands, four iridium(III) complexes (**PIQ-Ir1-me**, **PIQ-Ir2-cf3**, **PQZ-Ir3-me** and **PQZ-Ir4-cf3**) were synthesized and investigated. Due to the variation of the ligands, these Ir(III) complexes showed different emissions peaking from 602 to 628 nm with the phosphorescence quantum yields of 0.40–0.67. Moreover, applying these Ir(III) complexes as emitters, the organic light-emitting diodes (OLEDs) with the configuration of ITO/HATCN (hexaazatriphenylenehexacabonitrile, 5 nm)/TAPC (*bis*[4-(*N*,*N*-ditolylamino)-phenyl] cyclohexane, 50 nm)/Ir(III) complexes (8 wt%): TCTA (4,4′,4″-tri(9-carbazoyl)triphenylamine, 20 nm)/TmPyPB (1,3,5-tri[(3-pyridyl)-phen-3-yl]benzene, 40 nm)/LiF (1 nm)/Al (100 nm) exhibited good performances. Especially, the device with orange-red **PQZ-Ir4-cf3** emitter obtained the best device performances with the maximum current efficiency of 40.04 cd A^{-1} and the maximum power efficiency of 33.98 lm W^{-1}. For the pure red complex **PQZ-Ir4-me** with CIE coordinates at (0.64, 0.34) showed the maximum external quantum efficiency of 22.3%.

1. Introduction

Organic light-emitting diodes (OLEDs) with cyclometalated iridium(III) complexes as emitters have an extensive application in display panel and solid-state lighting in recent years [1–21], which is owing to their tunable emission colours and high internal quantum efficiency. To date, a large numbers of high efficient blue and green OLEDs have been developed by rational molecular design and the device architectures [22–29]. However, it is remain a great challenge to get high efficient red Ir(III) complexes as dopants in OLEDs [30–38]. It is well known that the energy gap is very important for the emission colour of the Ir(III) complexes [39–43]. Generally, increasing the π-conjugation of the main ligand in the Ir(III) complexes can narrow the energy gap and shift the emission colour to the red region [31,44–48]. For example, Liu et al. reported two deep-red cyclometalated Ir(III) complexes, in which fluorophenyl-isoquinoline derivatives (fpiq and $f_2$piq) were applied as the enlarged cyclometalated ligands, respectively [44]. In addition, Wang et al. reported two thiophenquinolone-based red Ir(III) complexes and obtained high efficient performances [45]. Moreover, Wang et al. developed high efficient Ir(III) complexes with furo[3,2 -c]pyridine ligand, and by adjusting the π-conjugation of the C-cheated blocks, the maximum emission peak of the Ir(III) complexes can be reached to 641 nm [46]. Furthermore, Yang et al. also reported some deep-red Ir(III) complexes based on 4-phenylthieno[3,2-c]quinolone ligand and phenanthridine derivatives with high external quantum efficiencies [47,48]. Therefore, it is an efficient strategy to achieve orange-red and red emission by introducing the enlarged main ligand in the Ir(III) complexes and rational design of the ancillary ligands.

Take this into consideration, four orange-red and red Ir(III) complexes **PIQ-Ir1-me**, **PIQ-Ir2-cf3, PQZ-Ir3-me** and **PQZ-Ir4-cf3** were synthesized and investigated, in which 1-(4-(trifluoromethyl)

* Corresponding author. State Key Laboratory of Coordination Chemistry, Collaborative Innovation Center of Advanced Microstructures, Jiangsu Key Laboratory of Advanced Organic Materials, Nanjing National Laboratory of Microstructures, School of Chemistry and Chemical Engineering, Nanjing University, Nanjing, 210093, PR China.
E-mail address: yxzheng@nju.edu.cn (Y.-X. Zheng).

https://doi.org/10.1016/j.jorganchem.2018.09.009
0022-328X/

phenyl)isoquinoline (tfmpiq) and 4-(4-(trifluoromethyl)phenyl)quinazoline (tfmpqz) were used as the main ligands, and 2-(3-methyl-1*H*-pyrazol-5-yl)pyridine (mepzpy), 2-(3-(trifluoromethyl)-1*H*-pyrazol-5-yl)pyridine (cf3pzpy) were applied as the ancillary ligands, respectively (Scheme 1). The introduction of tfmpiq and tfmpqz with a large π-conjugation systems could lead to a narrow energy gap of the Ir(III) complexes, therefore it can shift the emission into the red region. The with-drawing $-CF_3$ group in the main ligand is beneficial to increase steric hindrance of Ir(III) complexes and suppress triplet-triplet annihilation (TTA) and raise the yield of vacuum sublimation. Moreover, the lower vibrational frequency of the C–F bond can reduce the rate of radiationless deactivation, fluorination in the ligands can also increase the efficiency of the complexes and devices. Pyrazole pyridine derivatives (mepzpy and cf3pzpy) were denoted as ancillary ligands and expected that they can greatly influence the energy levels of the highest occupied molecular orbit (HOMO) and the lowest unoccupied molecular orbit (LUMO) of the Ir(III) complexes via the introduction of nitrogen atoms and affect the electron mobility and emission colours of the Ir(III) complexes [49–52]. As a result, the Ir(III) complexes exhibit different photoluminescent, electrochemical and electroluminescent performances due to the distinct molecular structures. Particularly, the device with **PQZ-Ir4-cf3** emitter showed the maximum current efficiency ($\eta_{c,max}$) of 40.04 cd A^{-1} and the maximum power efficiency ($\eta_{p,max}$) of 33.98 lm W^{-1} with Commission Internationale de 1′Eclairage (CIE) colour coordinates at (0.58, 0.40).

2. Experimental section

Scheme 1 shows the synthetic route of the Ir(III) complexes. The experimental details and the corresponding methods were clearly shown in Supporting Information (ESI). The synthesis of the ligands were according to our previous reports [53,54]. The μ-chloro-bridged dimers $[(tfmpiq)_2Ir(\mu\text{-}Cl)]_2$ and $[(tfmpqz)_2Ir(\mu\text{-}Cl)]_2$ were obtained according to general synthesis procedure [55]. All Ir(III) complexes were successfully synthesized by a two-step method and further purified by sublimation in vacuum [22,56,57]. The finally Ir(III) complexes were characterized by ^{1}H NMR, high resolution mass spectrometer (HRMS).

2.1. General synthesis of the Ir(III) complexes

The mixture of main ligand (tfmpiq or tfmpqz) (2.70 mmol) and $IrCl_3.3H_2O$ (0.38 g, 1.08 mmol) were refluxed in 2-ethoxyethanol (9 mL) and distilled water (3 mL) in N_2 atmosphere for 24 h. Then after adding of distilled water (50 mL), the red chloro-bridged dimmer precipitates ($[(tfmpiq)_2Ir(\mu\text{-}Cl)]_2$ or $[(tfmpqz)_2Ir(\mu\text{-}Cl)]_2$) were formed and collected, respectively. Then the suspension of the red chloro-bridged dimmer (0.83 mmol), the different ancillary ligands (2.07 mmol) and K_2CO_3 (0.95 g, 6.90 mmol) were refluxed in 2-ethoxyethanol (10 mL) overnight. Then the mixture was extracted with DCM (2 × 50 mL) and washed with distilled water (50 mL). After removing the organic solvent, the red solid was obtained by a flash silica gel column using petroleum ether (PE)/ethyl acetate (EA) (V/V = 1/5), then the red crystals were formed by further vacuum sublimation.

PIQ-Ir1-me (yield: 39%). ^{1}H NMR (400 MHz, $CDCl_3$) δ 8.98–8.90 (m, 1H), 8.87 (dd, *J* = 6.2, 3.4 Hz, 1H), 8.31 (t, *J* = 8.7 Hz, 2H), 7.88 (dd, *J* = 6.4, 3.1 Hz, 1H), 7.84 (dd, *J* = 6.1, 3.3 Hz, 1H), 7.76–7.72 (m, 3H), 7.71–7.69 (m, 2H), 7.67–7.60 (m, 2H), 7.58 (d, *J* = 6.4 Hz, 1H), 7.40 (dd, *J* = 8.7, 6.0 Hz, 2H), 7.28 (d, *J* = 6.8 Hz, 2H), 7.21 (dd, *J* = 8.4, 1.3 Hz, 1H), 6.86–6.78 (m, 1H), 6.65 (d, *J* = 1.2 Hz, 1H), 6.49 (s, 1H), 6.47 (s, 1H), 2.28 (s, 3H). HRMS (*m*/*z*): calcd for $C_{41}H_{27}F_6IrN_5$ $[M+H]^+$ 896.1800, found 896.1795.

PIQ-Ir2-cf3 (yield: 40%). ^{1}H NMR (400 MHz, $CDCl_3$) δ 8.98–8.92 (m, 1H), 8.88 (dd, *J* = 6.2, 3.4 Hz, 1H), 8.35–8.26 (m, 2H), 7.90 (dd, *J* = 6.3, 3.3 Hz, 1H), 7.87–7.82 (m, 1H), 7.78 (dd, *J* = 9.0, 5.4 Hz, 3H), 7.76–7.72 (m, 3H), 7.68 (d, *J* = 6.4 Hz, 1H), 7.49 (dd, *J* = 9.1, 6.0 Hz, 2H), 7.42 (d, *J* = 6.4 Hz, 1H), 7.29 (t, *J* = 7.7 Hz, 2H), 7.22 (d, *J* = 7.2 Hz, 1H), 7.04–6.95 (m, 2H), 6.67 (s, 1H), 6.43 (s, 1H). HRMS (*m*/*z*): calcd for $C_{41}H_{24}F_9IrN_5$ $[M+H]^+$ 950.1517, found 950.1514.

PQZ-Ir3-me (yield: 38%). ^{1}H NMR (400 MHz, $CDCl_3$) δ 8.89 (d, *J* = 8.5 Hz, 1H), 8.82 (d, *J* = 8.6 Hz, 1H), 8.47 (dd, *J* = 8.4, 2.9 Hz, 2H), 8.43 (s, 1H), 8.32 (s, 1H), 8.12 (d, *J* = 8.3 Hz, 1H), 8.07 (d, *J* = 7.9 Hz, 1H), 7.97–7.91 (m, 2H), 7.87–7.76 (m, 2H), 7.68 (s, 2H), 7.46 (d, *J* = 5.4 Hz, 1H), 7.35 (d, *J* = 7.2 Hz, 1H), 7.28 (s, 1H), 6.88 (s, 1H), 6.79 (s, 1H), 6.63 (s, 1H), 6.49 (s, 1H), 2.30 (d, *J* = 10.0 Hz, 3H). HRMS (*m*/*z*): calcd for $C_{39}H_{25}F_6IrN_7$ $[M+H]^+$ 898.1705, found 898.1701.

PQZ-Ir4-cf3 (yield: 32%). ^{1}H NMR (400 MHz, $CDCl_3$) δ 8.86 (dd,

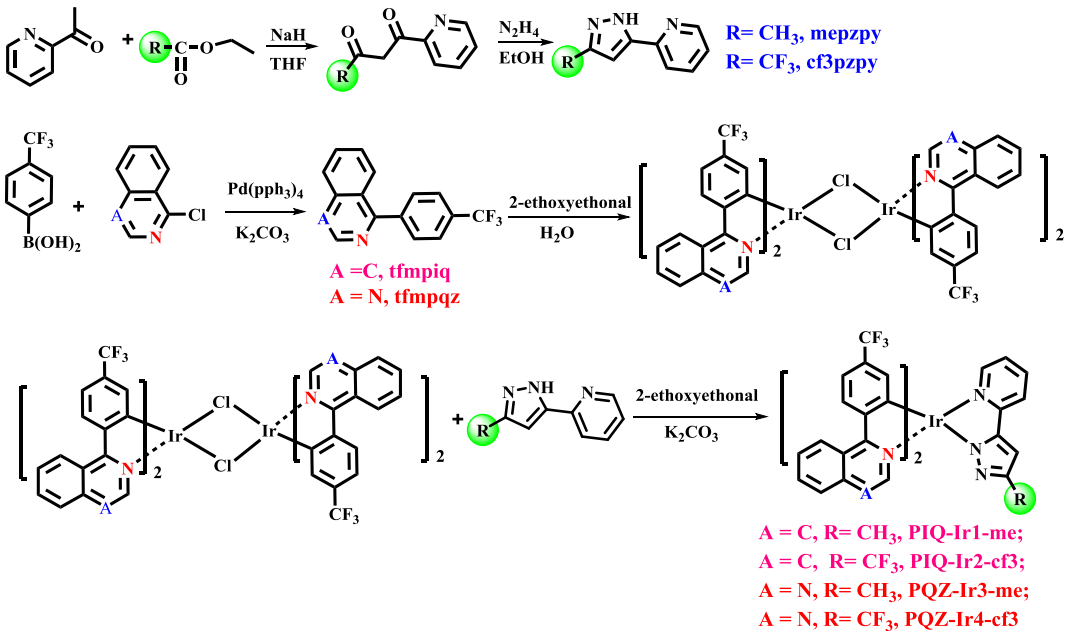

Scheme 1. Synthetic route of the Ir(III) complexes.

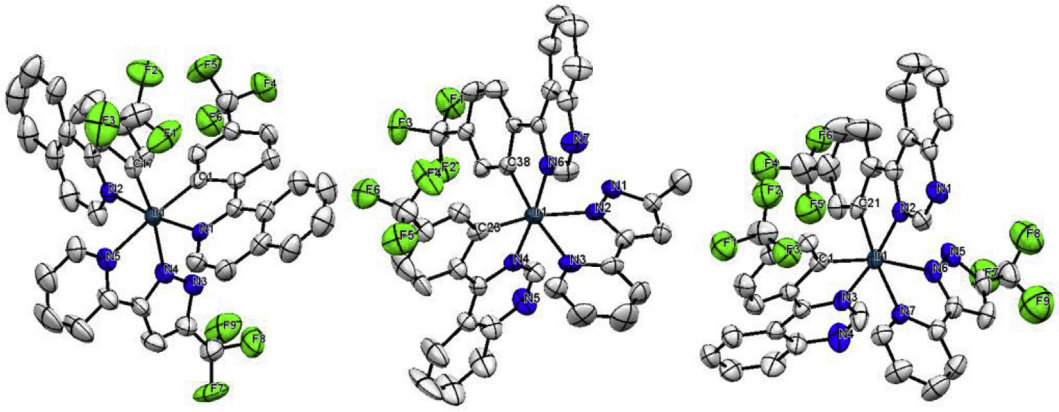

Fig. 1. ORTEP diagrams of **PIQ-Ir2-cf3** (CCDC No. 1819970), **PQZ-Ir3-me** (CCDC No. 1822137) and **PQZ-Ir4-cf3** (CCDC No. 1822164) complexes with the atom-numbering schemes. Hydrogen atoms are omitted for clarity. Ellipsoids are drawn at the 50% probability level.

J = 14.4, 8.6 Hz, 2H), 8.48 (dd, J = 18.3, 8.5 Hz, 2H), 8.38 (d, J = 9.4 Hz, 2H), 8.14 (d, J = 8.2 Hz, 1H), 8.07 (d, J = 8.1 Hz, 1H), 7.99–7.92 (m, 2H), 7.88–7.78 (m, 2H), 7.78–7.72 (m, 2H), 7.52 (d, J = 5.5 Hz, 1H), 7.38 (d, J = 8.5 Hz, 1H), 7.28 (s, 1H), 7.03–6.93 (m, 2H), 6.82 (s, 1H), 6.60 (s, 1H). HRMS (m/z): calcd for $C_{39}H_{22}F_9IrN_7$ $[M+H]^+$ 952.1422, found 952.1420.

3. Results and discussion

3.1. Complexes characterization

The molecular structures of **PIQ-Ir2-cf3, PQZ-Ir3-me** and **PQZ-Ir4-cf3** complexes were also determined by X-ray crystallography.

3.1.1. X-ray crystallographic analysis

The single crystals of **PIQ-Ir2-cf3, PQZ-Ir3-me and PQZ-Ir4-cf3** complexes were shown in Fig. 1, and the corresponding crystal information were displayed in Table 1. The selected bond lengths of the crystals were clearly depicted in Tables S1-S3 (ESI). The metal iridium atom adopts a three-dimensional spatial structure with two C^N main ligands and one N^N ancillary ligand. More interestingly, the bond lengths of Ir1–N4 (2.120 (4) Å) and Ir1–N5 (2.173 (4) Å) in ancillary ligand of **PIQ-Ir2-cf3** complex are longer than those of Ir1–N1 (2.041 (4) Å) and Ir1–N2 (2.039 (4) Å) in main ligand, respectively. And the others exhibited the similarity. This phenomenon is attributed to the carbons' sigma donation (*trans effect*) of the Ir(III) complexes [58–61].

3.1.2. Thermal property

The Ir(III) complexes with good thermal properties are very important for the OLEDs fabrication. If a complex can be applied in practical OLEDs, the decomposition temperature (T_d) need to be high enough to guarantee that the complex could be deposited onto the solid face without any decomposition on sublimation. From the recorded thermogravimetric analysis (TGA) curves of the Ir(III) complexes in Fig. 2 it can be observed that all complexes have high T_ds range from 379 to 393 °C (with 5% loss of weight, Table 2), which are beneficial for their OLEDs application.

Table 1
Crystal information of **PIQ-Ir2-cf3**, **PQZ-Ir3-me** and **PQZ-Ir4-cf3** complexes.

	PIQ-Ir2-cf3	**PQZ-Ir3-me**	**PQZ-Ir4-cf3**
Formula	$C_{41}H_{23}F_9IrN_5$	$C_{39}H_{24}F_6IrN_7$	$C_{39}H_{21}F_9IrN_7$
Formula weight	948.84	896.85	950.83
T (K)	296 (2)	296 (2)	296 (2)
Wavelength (Å)	0.71073	0.71073	0.71073
Crystal system	Monoclinic	Monoclinic	Monoclinic
Space group	$C2/c$	$P2_1/n$	$P2_1/c$
a (Å)	22.792 (5)	12.0808 (18)	19.3754 (15)
b (Å)	12.154 (3)	15.430 (2)	14.2393 (11)
c (Å)	25.929 (7)	18.858 (3)	13.1682 (10)
α (deg)	90.00	90.00	90.00
β (deg)	93.894 (5)	103.163 (3)	94.6480 (10)
γ (deg)	90.00	90.00	90.00
V (Å^3)	7166 (3)	3423.0 (9)	3621.1 (5)
Z	8	4	4
ρ_{calcd} (g/cm^3)	1.759	1.740	1.744
μ (Mo Kα) (mm^{-1})	3.812	3.974	3.774
F (000)	3696	1752	1848
Range of transm factors (deg)	1.791–25.009	1.724–25.000	1.054–25.010
Reflns collected	19753	18795	19789
Unique(R_{int})	6333 (0.0611)	6021 (0.0723)	6382 (0.0293)
R_1^a, wR_2^b [I > 2s(I)]	0.0340, 0.0683	0.0409, 0.0903	0.0372, 0.0985
R_1^a, wR_2^b (all data)	0.0552, 0.0764	0.0687, 0.1049	0.0478, 0.1053
GOF on F^2	0.977	0.988	1.096
CCDC No.	1819970	1822137	1822164

$R_1^a = \Sigma||F_o| - |F_c||/\Sigma F_o|$. $wR_2^b = [\Sigma w(F_o^2 - F_c^2)^2/\Sigma w(F_o^2)]^{1/2}$.

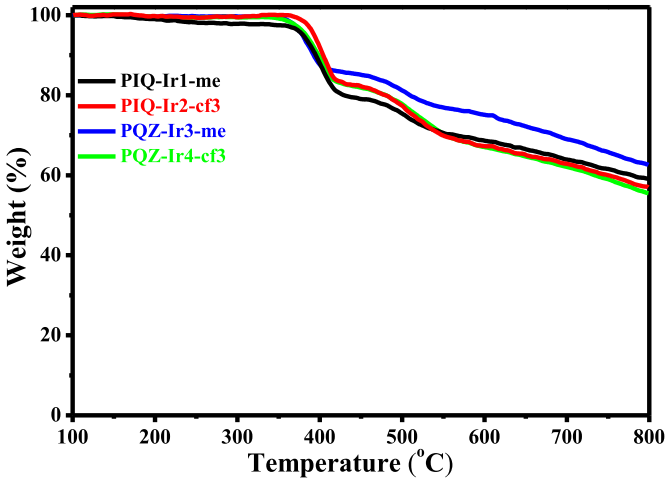

Fig. 2. The TGA curves of the Ir(III) complexes.

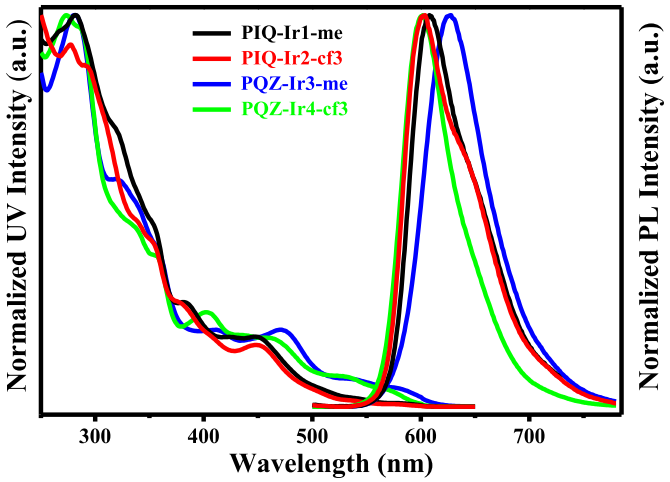

Fig. 3. Normalized UV/vis absorption and emission spectra of the Ir(III) complexes in dilute DCM (10^{-5} M) at RT.

3.2. Photophysical properties

Fig. 3 showed the UV/vis absorption spectra of the Ir(III) complexes in degassed dichloromethane (DCM) (10^{-5} M) at room temperature (RT), and the corresponding data are also summarized in Table 2. The Ir(III) complexes showed similar absorption spectra ranged from 250 to 600 nm. The high-lying absorptions under 350 nm are mainly ascribed to π-π* transitions of the ligands. While the lower absorptions (400–600 nm) are attributed to the ^{1}MLCT and ^{3}MLCT (metal-to-ligand charge transfer) excited states or LLCT (ligand-to-ligand charge transfer) transition coming from spin-orbit coupling effect of iridium atom. Obviously, compared with the Ir(III) complexes **PIQ-Ir1-me** and **PIQ-Ir2-cf3** that using 1-(4-(trifluoromethyl)phenyl)-isoquinoline as the main ligand, the Ir(III) complexes **PQZ-Ir3-me** and **PQZ-Ir4-cf3** based on 4-(4-(trifluoromethyl)phenyl)quinazoline main ligand exhibited more red-shifted absorption peaks between 450 and 600 nm, which indicated that it is an efficient method to obtain red-shifted absorption by introducing nitrogen atom into the main ligand of the Ir(III) complexes.

Fig. 3 also shows the photoluminescence (PL) spectra of the Ir(III) complexes in DCM (10^{-5} M) at RT. All Ir(III) complexes exhibited emissions peaks from 602 to 628 nm (Table 2), which are in the orange-red and red region. Obviously, **PIQ-Ir2-cf3** and **PQZ-Ir4-cf3** with trifluoromethyl unit in the ancillary ligands displayed blue-shifted emission peaked at 604 and 602 nm, while **PIQ-Ir1-me** and **PQZ-Ir3-me** with ancillary ligands attached methyl group showed red-shifted PL emission at 608 and 628 nm, respectively, which indicated that the different substituents in the ancillary ligands have a great effect on the emission.

Furthermore, the Ir(III) complexes showed high phosphorescence quantum yields in the range of 0.40–0.67. It is observed that though the change of the main ligand has no obvious effect on their emission colour, the photoluminescence efficiencies of **PQZ-Ir3-me** ($\Phi_{PL} = 0.60$) and **PQZ-Ir4-cf3** ($\Phi_{PL} = 0.67$) are higher than that of **PIQ-Ir1-me** ($\Phi_{PL} = 0.40$) and **PIQ-Ir2-cf3** ($\Phi_{PL} = 0.41$), which indicated that the different main ligands have a great influence on their Φ_{PL} and one more N atom in the main ligand can improve the PL efficiency greatly. According to the reported reference [62], one more N electronegative atom in the main ligand tfmpqz of iridium complex disturbs the electron density of the ligand, resulting in a decrease in the energy band gap of iridium complex and the bathochromic shift. Therefore, the N electronegative atom effect of tfmpqz in iridium complex have facilitated improved Φ_{PL} than the iridium complex based on tfmpiq. Generally, the excited lifetime (τ_p) of Ir(III) complexes is also important for determining of triplet-triplet annihilation (TTA) effect [63,64]. In this case, the τ_p values of four Ir(III) complexes measured in DCM ranged from 2.06 to 2.21 μs (Table 2). All these results clearly demonstrated that the four novel Ir(III) complexes are efficient candidates in OLEDs applications.

3.3. Electrochemical property and theoretical calculations

It is well known that the HOMO and LUMO energy levels (E_{HOMO}/E_{LUMO}) are significant for the OLEDs device design and fabrication. Therefore, to calculate the E_{HOMO}/E_{LUMO} values of these complexes, cyclic voltammetry (CV) properties were measured and displayed in Fig. S1 (ESI). According to the oxidation potentials of the Ir(III) complexes recorded by the CV curves and the empirical equation: $E_{HOMO} = -(E_{ox} + 4.8)$ eV, $E_{LUMO} = E_g^{opt} + E_{HOMO}$, their E_{HOMO} and E_{LUMO} values can be calculated, respectively. And the CV data are collected in Table 2 and Table S4 (ESI). Compared to the Ir(III) complexes **PIQ-Ir1-me** and **PQZ-Ir3-me** with mepzpy as the ancillary ligand, **PIQ-Ir2-cf3** and **PQZ-Ir4-cf3** complexes with

Table 2
Photophysical data of the Ir(III) complexes.

Complexes	T_d (°C)	UV[a] (nm)	PL (nm)[a]	Φ_{PL}[b]	τ_p[c] (μs)	E_{HOMO} (eV)[d]	E_{LUMO} (eV)[e]
PIQ-Ir1-me	380	281,386,453	608	0.40	2.12	−5.49	−3.24
PIQ-Ir2-cf3	393	276,380,452	604	0.41	2.21	−5.72	−3.47
PQZ-Ir3-me	379	282,321,474	628	0.60	2.06	−5.51	−3.53
PQZ-Ir4-cf3	383	272,404,464	602	0.67	2.09	−5.97	−3.99

[a] Measured in degassed DCM (10^{-5} M) at RT.
[b] Measured in degassed DCM (10^{-5} M) in N_2 atmosphere according to the equation of $\Phi_s = \Phi_r(\eta_s^2 A_r I_s / \eta_r^2 A_s I_r)$.
[c] Measured in degassed DCM (10^{-5} M) in N_2 atmosphere.
[d] Calculated from empirical equation: $E_{HOMO} = -(E_{ox} + 4.8)$ eV.
[e] Calculated from $E_{LUMO} = E_g^{opt} + E_{HOMO}$.

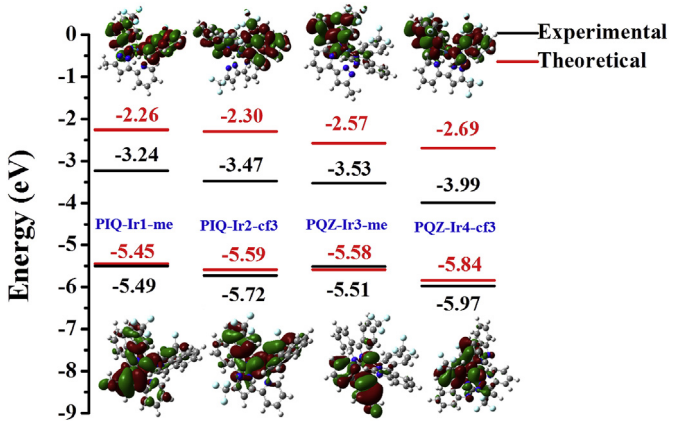

Fig. 4. Theoretical (red) and experimental (black, determined by cyclic voltammetry measurement) HOMO/LUMO energy levels of the Ir(III) complexes. (For interpretation of the references to colour in this figure legend, the reader is referred to the Web version of this article.)

trifluoromethyl group in the ancillary ligands own a relative low E_{HOMO} values, which indicated that the introduction of withdrawing trifluoromethyl group to the ancillary ligand takes a great impact on electrochemical properties of Ir(III) complexes. The results are also agree with the emission peaks sequence of these complexes.

Moreover, density functional theory (DFT) calculations were conducted to further research the orbital distributions of the Ir(III) complexes. Fig. 4 clearly showed their optimized HOMO and LUMO structures, and the HOMO and LUMO distributions of each fragment of Ir(III) complexes are displayed in Table S5 (ESI). Similarly with other reported Ir(III) complexes, the LUMOs are mainly scattered in main ligands (tfmpiq or tfmpqz) with a high proportion (93.20%–95.19%) (Table S5), but the HOMOs distributions have a great dependence on the ancillary ligands. For example, the HOMOs of the Ir(III) complexes (**PIQ-Ir1-me** and **PQZ-Ir3-me**) are mainly located in metal iridium atom and mepzpy ancillary ligand, and mepzpy own the HOMO energy proportion of 35.89% and 63.95%, respectively. While the Ir(III) complexes **PIQ-Ir2-cf3** and **PQZ-Ir4-cf3** with cf3pzpy as ancillary ligand have the similar HOMOs distributions into the main ligands and iridium atoms with the almost same proportion. Due to the contributions of different ancillary ligands to the HOMO energies levels, the Ir(III) complexes display distinct PL emissions, and **PQZ-Ir3-me** complex exhibited the maximum PL emission at 628 nm. Moreover, the ancillary ligand mepzpy of **PQZ-Ir3-me** complexes accounted for a largest HOMO energy proportion, but cf3pzpy of **PIQ-Ir2-cf3** and **PQZ-Ir4-cf3** complexes have almost no HOMO energy distributions. This also explain why **PQZ-Ir3-me** complex could achieve the maximum PL emission at 628 nm. Therefore, it is important for the Ir(III) complexes to obtain red-shifted PL emissions by the introduction of nitrogen atom into the main ligand and rational design of the ancillary ligands with a large HOMO energy proportions. These results indicate that different ancillary ligands could take a distinct influence on the HOMO energy levels of the Ir(III) complexes and further influence the PL emissions in various degree, which are well matched with our design strategy.

3.4. Electroluminescent property

To explore the electroluminescence properties of the Ir(III) complexes, the OLEDs with the structure of ITO/HATCN (hexaazatriphenylenehexacabonitrile, 5 nm)/TAPC (bis[4-(*N*,*N*-ditolylamino)-phenyl]cyclohexane, 50 nm)/Ir complexes (8 wt%): TCTA (4,4′,4″-tri(9-carbazoyl)triphenylamine, 20 nm)/TmPyPB (1,3,5-tri[(3-pyridyl)-phen-3-yl]benzene, 40 nm)/LiF (1 nm)/Al (100 nm) were fabricated (Scheme 2). Conveniently, the devices with **PIQ-Ir1-me, PIQ-Ir2-cf3**, **PQZ-Ir3-me** and **PQZ-Ir4-cf3** complexes as dopants are named G1, G2, G3 and G4, respectively. HATCN and TAPC were applied as hole-injection layer and hole-transporting layer, while LiF and TmPyPB were utilized as electron-injection and electron-transporting layer, respectively. In addition, TCTA was applied as host material owing to its good hole-transporting ability.

Fig. 5 depicts the EL spectra, luminance (*L*) *versus* voltage (V), current efficiency (η_c) *versus* luminance, and external quantum efficiency (EQE) *versus* luminance properties of the devices, and the important EL data of devices G1- G4 were summarized in Table 3. Fig. 5a clearly depicted that the EL emissions for device G1 - G4 showed a little blue-shifted main peaks at 592–618 nm at the optimized 8 wt% doping concentration compared with the PL emissions of these Ir(III) complexes in DCM at RT. Furthermore, all devices exhibited weak emission peaks of the host material at 397 nm, which is attributed to incomplete energy transfer between the host material and the Ir(III) complexes. The CIE coordinates of the G1 - G4 devices were calculated at (0.63, 0.36), (0.60, 0.36), (0.64, 0.34) and (0.58, 0.40), respectively, exhibiting orange-red and red emissions.

Due to their similar molecular structures, it is found that the

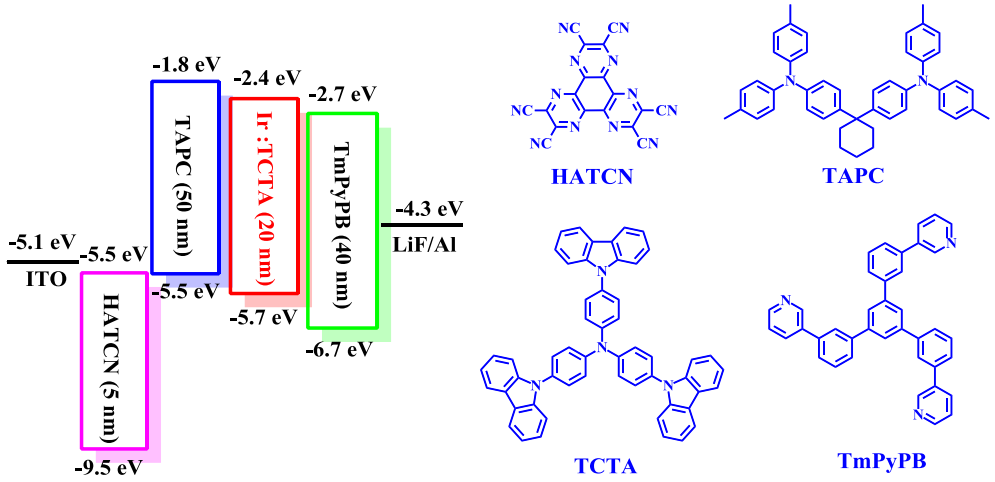

Scheme 2. The OLEDs device structure and their molecular structures used in this work.

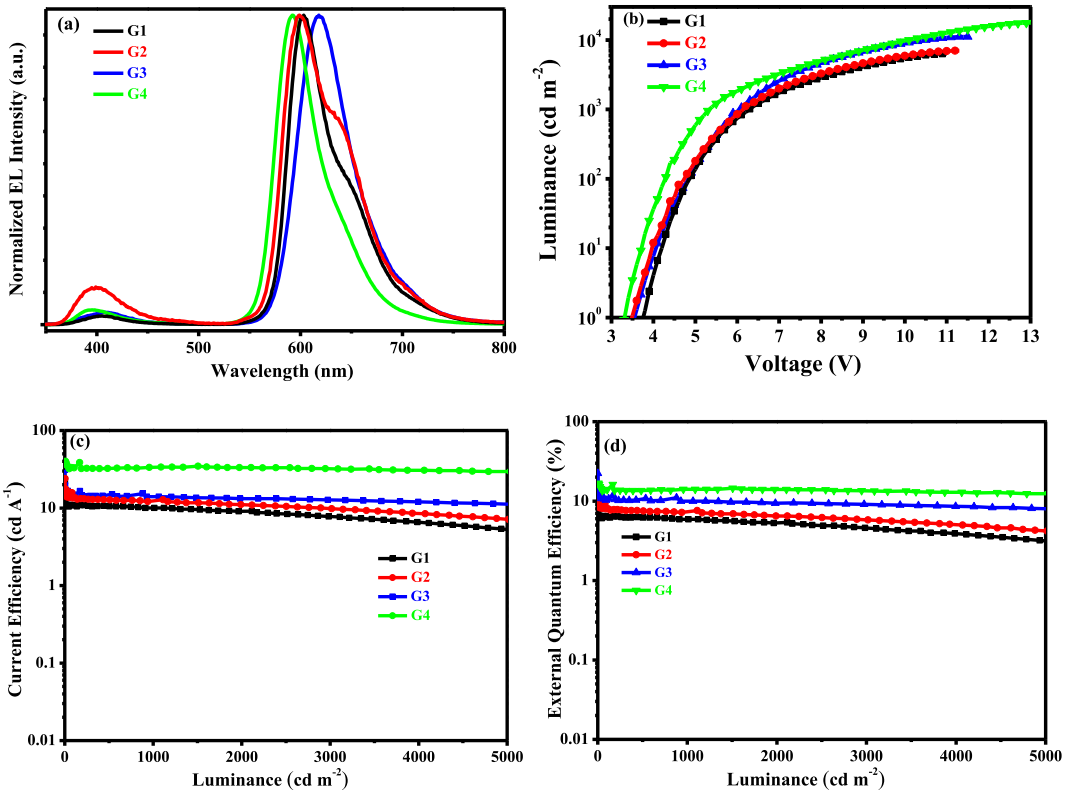

Fig. 5. Characteristics of devices with configuration of ITO/HATCN (5 nm)/TAPC (50 nm)/TCTA: Ir(III) complexes (20 nm, 8 wt%)/TmPyPB (40 nm)/LiF (1 nm)/Al (100 nm): (a) EL spectra; (b) *L*-V curves; (c)η_c-*L* curves; (d) EQE -*L* curves for G1-G4.

Table 3
Key EL data of devices G1- G4.

Devices (8 wt%)	V_{on} (V)[a]	λ_{EL} (nm)	L_{max} (cd m^{-2})[b]	$\eta_{c,max}$ (cd A^{-1})[c]	$\eta_{p,max}$ (lm W^{-1})[d]	EQE_{max} (%)[e]	CIE (x,y)
G1	3.7	603	6343	23.52	19.43	13.9	(0.63,0.36)
G2	3.5	599	7023	23.99	20.36	14.2	(0.60,0.36)
G3	3.5	618	11156	31.15	26.44	22.3	(0.64,0.34)
G4	3.3	592	17745	40.04	33.98	16.8	(0.58,0.40)

[a] Turn-on voltage, the driving voltage at 1 cd m^{-2}.
[b] Maximum luminance.
[c] Current efficiency.
[d] Power efficiency.
[e] External quantum efficiency calculated within visible spectrum region.

device performances are mainly determined by the phosphorescence quantum yield (Φ_{PL}) of the Ir(III) complexes and possible better electron mobility of tfmpqz based complexes, which have another N atom in the main ligand. For example, From Fig. 5b-d, it is observed that the device G1 doping with **PIQ-Ir1-me** complex ($\Phi_{PL} = 0.40$) shows the lowest device performances with the maximum luminance (L_{max}) of 6343 cd m^{-2}, the maximum current efficiency ($\eta_{c,max}$) of 23.52 cd A^{-1}, the maximum external quantum efficiency (EQE_{max}) of 13.9% and the maximum power efficiency ($\eta_{p,max}$) of 19.43 lm W^{-1}. Due to the almost same Φ_{PL} of **PIQ-Ir2-cf3** complex ($\Phi_{PL} = 0.41$), the G2 device exhibit the L_{max} of 7023 cd m^{-2}, the $\eta_{c,max}$ of 23.99 cd A^{-1}, the EQE_{max} of 14.2% and the $\eta_{p,max}$ of 20.36 lm W^{-1}. Because the **PQZ-Ir4-cf3** complex has the highest Φ_{PL} of 0.67, the device G4 shows the best performances with the L_{max} of 17,745 cd m^{-2}, the $\eta_{c,max}$ of 40.04 cd A^{-1}, the EQE_{max} of 16.8% and the $\eta_{p,max}$ of 33.98 lm W^{-1}. Due to the little lower Φ_{PL} of **PQZ-Ir3-me** complex ($\Phi_{PL} = 0.60$), the device G3 also exhibited the relatively lower device performances with the $\eta_{c,max}$ of 31.15 cd A^{-1}, the $\eta_{p,max}$ of 26.44 lm W^{-1}, the EQE_{max} of 22.3% and the L_{max} of 11,156 cd m^{-2}. It is worth noting that though the G3 device shows a relatively lower current efficiency than that of device G4, the maximum external quantum efficiency is the highest (22.3%), which is mainly due to the red-shifted EL emission. In general, most photo-detectors used in OLEDs research are sensitive to the green light and the EL emission in red region always show lower current efficiency value [65]. Obviously, the Ir(III) complexes with tfmpqz as main ligands have a good advantage on OLEDs performances, such as lower turn-on voltage, higher luminance and current efficiency, which proves that the importance of nitrogen atoms in the main ligand.

4. Conclusion

In summary, with 1-(4-(trifluoromethyl)phenyl)isoquinoline (tfmpiq) and 4-(4-(trifluoromethyl)phenyl)quinazoline (tfmpqz) as the main ligands and pyrazole pyridine derivatives as the ancillary ligands, four orange-red and red Ir(III) complexes with quantum yields up to 0.67 were synthesized, respectively. The devices doping

with these Ir(III) complexes as emitters showed the EL emission peaks at 592–618 nm. Furthermore, the device using **PQZ-Ir4-cf3** complex as dopant achieved the best performances with the maximum current efficiency of 40.04 cd A^{-1} and the maximum power efficiency of 33.98 lm W^{-1}, respectively. For the pure red complex **PQZ-Ir3-me** with CIE coordinates at (0.64, 0.34), its device showed the maximum external quantum efficiency of 22.3%. This research found that the Ir(III) complexes have a red-shifted PL emissions and improved OLEDs performances by introduction of nitrogen atoms into main ligand and pyrazole pyridine derivatives as ancillary ligands, which suggests an efficient method to obtain highly efficient orange-red and red Ir(III) complexes for OLEDs.

Acknowledgments

This work was supported by the National Natural Science Foundation of China (51773088), the Natural Science Foundation of Jiangsu Province (BY2016075-02) and the Fundamental Research Funds for the Central Universities (020514380131).

Appendix A. Supplementary data

Supplementary data to this article can be found online at https://doi.org/10.1016/j.jorganchem.2018.09.009.

References

[1] D. Liu, L. Deng, W. Li, R. Yao, D. Li, M. Wang, S. Zhang, Novel Ir(ppy)$_3$ derivatives: simple structure modification toward nearly 30% external quantum efficiency in phosphorescent organic light-emitting diodes, Adv. Opt. Mater. 4 (2016) 864–870.
[2] D. Ma, T. Tsuboi, Y. Qiu, L. Duan, Recent progress in ionic iridium(III) complexes for organic electronic devices, Adv. Mater. 29 (2017) 1603253.
[3] Y. Zheng, A.S. Batsanov, M.A. Fox, H.A. Al-Attar, K. Abdullah, V. Jankus, M.R. Bryce, A.P. Monkman, Bimetallic cyclometalated iridium(III) diastereomers with non-innocent bridging ligands for high-efficiency phosphorescent OLEDs, Angew. Chem. Int. Ed. 53 (2014) 11616–11619.
[4] J. Zhang, L. Zhou, H.A. Al-Attar, K. Shao, L. Wang, D. Zhu, Efficient light-emitting electrochemical cells (LECs) based on ionic iridium(III) complexes with 1,3,4-oxadiazole ligands, Adv. Funct. Mater. 23 (2013) 4667–4677.
[5] C. Shi, H. Sun, X. Tang, W. Lv, H. Yan, Q. Zhao, Variable photophysical properties of phosphorescent iridium(III) complexes triggered by closo- and nido-carborane substitution, Angew. Chem. Int. Ed. 52 (2013) 13434–13438.
[6] P. Brulatti, R.J. Gildea, J.A. Howard, V. Fattori, M. Cocchi, J.A. Williams, Luminescent iridium(III) complexes with N^C^N-coordinated terdentate ligands: dual tuning of the emission energy and application to organic light-emitting devices, Inorg. Chem. 51 (2012) 3813–3826.
[7] C.H. Chang, Z.J. Wu, C.H. Chiu, Y.H. Liang, Y.S. Tsai, J.L. Liao, A new class of sky-blue-emitting Ir(III) phosphors assembled using fluorine-free pyridyl pyrimidine cyclometalates: application toward high-performance sky-blue- and white-emitting OLEDs, ACS Appl. Mater. Interfaces 5 (2013) 7341–7351.
[8] J.M. Fernandez-Hernandez, J.I. Beltran, V. Lemaur, M.D. Galvez-Lopez, C.H. Chien, F. Polo, Iridium(III) emitters based on 1,4-disubstituted-1H-1,2,3-triazoles as cyclometalating ligand: synthesis, characterization, and electroluminescent devices, Inorg. Chem. 52 (2013) 1812–1824.
[9] S. Lee, S.O. Kim, H. Shin, H.J. Yun, K. Yang, S.K. Kwon, Deep-blue phosphorescence from perfluoro carbonyl-substituted iridium complexes, J. Am. Chem. Soc. 135 (2013) 14321–14328.
[10] N.M. Shavaleev, G. Xie, S. Varghese, D.B. Cordes, A.M. Slawin, C. Momblona, Green phosphorescence and electroluminescence of sulfur pentafluoride-functionalized cationic iridium(III) complexes, Inorg. Chem. 54 (2015) 5907–5914.
[11] X. Yang, G. Zhou, W.Y. Wong, Functionalization of phosphorescent emitters and their host materials by main-group elements for phosphorescent organic light-emitting devices, Chem. Soc. Rev. 44 (2015) 8484–8575.
[12] X. Xu, X. Yang, J. Zhao, G. Zhou, W.Y. Wong, Recent advances in solution-processable dendrimers for highly efficient phosphorescent organic light-emitting diodes (PHOLEDs), Asian J. Org. Chem. 4 (2015) 394–429.
[13] L. Ying, C.L. Ho, H. Wu, Y. Cao, W.Y. Wong, White polymer light-emitting devices for solid-state lighting: materials, devices, and recent progress, Adv. Mater. 26 (2014) 2459–2473.
[14] C.L. Ho, H. Li, W.Y. Wong, Red to near-infrared organometallic phosphorescent dyes for OLED applications, J. Organomet. Chem. 751 (2014) 261–285.
[15] G. Tan, S. Chen, N. Sun, Y. Li, D. Fortin, W.Y. Wong, Highly efficient iridium(III) phosphors with phenoxy-substituted ligands and their high-performance OLEDs, J. Mater. Chem. C. 1 (2013) 808–821.
[16] X. Yang, G. Zhou, W.Y. Wong, Recent design tactics for high performance white polymer light-emitting diodes, J. Mater. Chem. C. 2 (2014) 1760.
[17] W.Y. Wong, C.L. Ho, Functional metallophosphors for effective charge Carrier injection/transport: new robust OLED materials with emerging applications, J. Mater. Chem. 19 (2009) 4457–4482.
[18] W.Y. Wong, C.L. Ho, Heavy metal organometallic electrophosphors derived from multi-component chromophores, Coord. Chem. Rev. 253 (2009) 1709–1758.
[19] G.J. Zhou, W.Y. Wong, S. Suo, Recent progress and current challenges in phosphorescent white organic light-emitting diodes (WOLEDs), J. Photochem. Photobiol. C Photochem. Rev. 11 (2010) 133–156.
[20] G. Zhou, W.Y. Wong, X. Yang, New design tactics in OLEDs using functionalized 2-phenylpyridine-type cyclometalates of iridium(III) and platinum(II), Chem. Asian J. 6 (2011) 1706–1727.
[21] Cheuk-Lam Ho, Wai-Yeung Wong, Charge and energy transfers in functional metallophosphors and metallopolyynes, Coord. Chem. Rev. 257 (2013) 1614–1649.
[22] Q.L. Xu, X. Liang, S. Zhang, Y.M. Jing, X. Liu, G.Z. Lu, Efficient OLEDs with low efficiency roll-off using iridium complexes possessing good electron mobility, J. Mater. Chem. C. 3 (2015) 3694–3701.
[23] J. Jayabharathi, V. Thanikachalam, R. Sathishkumar, Highly phosphorescent green emitting iridium(III) complexes for application in OLEDs, New J. Chem. 39 (2015) 235–245.
[24] Y. Li, L. Zhou, Y. Jiang, R. Cui, X. Zhao, Y. Zheng, Green organic light-emitting devices with external quantum efficiency up to nearly 30% based on an iridium complex with a tetraphenylimidodiphosphinate ligand, RSC Adv. 6 (2016) 63200–63205.
[25] D. Ma, C. Zhang, Y. Qiu, L. Duan, Highly efficient blue-green organic light-emitting diodes achieved by controlling the anionic migration of cationic iridium(III) complexes, J. Mater. Chem. C. 4 (2016) 5731–5738.
[26] Y.M. Jing, Y.X. Zheng, J.L. Zuo, Efficient green electroluminescence based on an iridium(III) complex with different device structures, RSC Adv. 7 (2017) 2615–2620.
[27] J.H. Zhao, Y.X. Hu, Y. Dong, X. Xia, H.J. Chi, G.Y. Xiao, Novel bluish green benzimidazole-based iridium(III) complexes for highly efficient phosphorescent organic light-emitting diodes, New J. Chem. 41 (2017) 1973–1979.
[28] A. Liang, J. Tang, P. Cai, X. Yang, W. Wu, L. Chen, Sky-blue phosphorescent organic light-emitting diodes with dibenzo-24-crown-8 substituted iridium(III) complexes as the dopants, Dyes Pigments 138 (2017) 77–82.
[29] Q.L. Xu, X. Liang, L. Jiang, Y. Zhao, Y.X. Zheng, Two blue iridium complexes for efficient electroluminescence with low efficiency roll-off, RSC Adv. 5 (2015) 89218–89225.
[30] L. Zhao, S. Wang, J. Lü, J. Ding, L. Wang, Solution processable red iridium dendrimers containing oligocarbazole dendrons for efficient nondoped and doped phosphorescent OLEDs, J. Mater. Chem. C. 5 (2017) 9753–9760.
[31] X. Yang, X. Xu, J.S. Dang, G. Zhou, C.L. Ho, W.Y. Wong, From mononuclear to dinuclear iridium(III) complex: effective tuning of the optoelectronic characteristics for organic light-emitting diodes, Inorg. Chem. 55 (2016) 1720–1727.
[32] C.L. Ho, W.Y. Wong, Q. Wang, D. Ma, L. Wang, Z. Lin, A Multifunctional iridium-carbazolyl orange phosphor for high-performance two-element WOLED exploiting exciton-managed fluorescence/phosphorescence, Adv. Funct. Mater. 18 (2008) 928–937.
[33] X. Liu, B. Yao, Z. Zhang, X. Zhao, B. Zhang, W.Y. Wong, Y. Cheng, Z. Xie, Power-efficient solution-processed red organic light-emitting diodes based on an exciplex host and a novel phosphorescent iridium complex, J. Mater. Chem. C 4 (2016) 5787–5794.
[34] X. Liu, B. Yao, H. Wang, B. Zhang a, X. Lin, X. Zhao, Y. Cheng, Z. Xie, W.Y. Wong, Efficient solution-processed yellow/orange phosphorescent OLEDs based on heteroleptic Ir(III) complexes with 2-(9,9-diethylfluorene-2-yl)pyridine main ligand and various ancillary ligands, Org. Electron. 54 (2018) 197–203.
[35] X. Yin, T. Zhang, Q. Peng, T. Zhou, W. Zeng, Z. Zhu, G. Xie, F. Li, D. Ma, C. Yang, Benzobisoxazole-based electron transporting materials with high T g and ambipolar property: high efficiency deep-red phosphorescent OLEDs, J. Mater. Chem. C 3 (2015) 7589–7596.
[36] M. Zhu, Y. Li, B. Jiang, S. Gong, H. Wu, J. Qin, Y. Cao, C. Yang, Efficient saturated red electrophosphorescence by using solution- processed 1-phenylisoquinoline-based iridium phosphors with peripheral functional encapsulation, Org. Electron. 26 (2015) 400–407.
[37] C. Fan, C. Yang, Yellow/orange emissive heavy-metal complexes as phosphors in monochromatic and white organic light-emitting devices, Chem. Soc. Rev. 43 (2014) 6439–6469.
[38] C. Fan, J. Miao, B. Jiang, C. Yang, H. Wu, J. Qin, Y. Cao, Highly efficient, solution-processed orange–red phosphorescent OLEDs by using new iridium phosphor with thieno[3,2-c] pyridine derivative as cyclometalating ligand, Org. Electron. 14 (2013) 3392–3398.
[39] P. Tao, Y. Zhang, J. Wang, L. Wei, H. Li, X. Li, Highly efficient blue phosphorescent iridium(III) complexes with various ancillary ligands for partially solution-processed organic light-emitting diodes, J. Mater. Chem. C. 5 (2017) 9306–9314.
[40] N. Okamura, T. Maeda, S. Yagi, Sky-blue phosphorescence from bis- and tris-cyclometalated iridium(III) complexes bearing carbazole-based dendrons: fabrication of non-doped multilayer organic light-emitting diodes by solution processing, New J. Chem. 41 (2017) 10357–10366.
[41] S.K. Kang, J. Jeon, S.H. Jin, Y.I. Kim, Orange-yellow phosphorescent iridium(III)

complex for solution-processed organic light-emitting diodes: structural, optical and electroluminescent properties of bis(2-phenylbenzothiazole)[2-(2-hydroxyphenyl)benzothiazole]iridium(III), Bull. Kor. Chem. Soc. 38 (2017) 646–650.
[42] H. Cao, G. Shan, X. Wen, H. Sun, Z. Su, R. Zhong, An orange iridium(III) complex with wide-bandwidth in electroluminescence for fabrication of high-quality white organic light-emitting diodes, J. Mater. Chem. C. 1 (2013) 7371.
[43] V. Cherpak, P. Stakhira, B. Minaev, G. Baryshnikov, E. Stromylo, I. Helzhynskyy, Efficient "warm-white" OLEDs based on the phosphorescent bis-cyclometalated iridium(III) complex, J. Phys. Chem. C 118 (2014) 11271–11278.
[44] G. Li, P. Li, X. Zhuang, K. Ye, Y. Liu, Y. Wang, Rational design and characterization of heteroleptic phosphorescent complexes for highly efficient deep-red organic light-emitting devices, ACS Appl. Mater. Interfaces 9 (2017) 11749–11758.
[45] Y. Miao, P. Tao, K. Wang, H. Li, B. Zhao, L. Gao, H. Wang, Highly efficient red and white organic light-emitting diodes with external quantum efficiency beyond 20% by employing pyridylimidazole-based metallophosphors, ACS Appl. Mater. Interfaces 9 (2017) 37873–37882.
[46] Z. Yan, Y. Wang, J. Ding, Y. Wang, L. Wang, Highly efficient phosphorescent furo[3,2-c]pyridine based iridium complexes with tunable emission colors over the whole visible range, ACS Appl. Mater. Interfaces 10 (2018) 1888–1896.
[47] B. Jiang, Y. Gu, J. Qin, X. Ning, S. Gong, G. Xie, Deep-red iridium(III) complexes cyclometalated by phenanthridine derivatives for highly efficient solution-processed organic light-emitting diodes, J. Mater. Chem. C. 4 (2016) 3492–3498.
[48] B. Jiang, X. Ning, S. Gong, N. Jiang, C. Zhong, Z.H. Lu, Highly efficient red iridium(III) complexes cyclometalated by 4-phenylthieno[3,2-c]quinoline ligands for phosphorescent OLEDs with external quantum efficiencies over 20%, J. Mater. Chem. C. 5 (2017) 10220–10224.
[49] C.H. Yang, S.W. Li, Y. Chi, Y.M. Cheng, Y.S. Yeh, P.T. Chou, Heteroleptic cyclometalated iridium(III) complexes displaying blue phosphorescence in solution and solid state at room temperature, Inorg. Chem. 44 (2005) 7770–7780.
[50] S.Y. Chang, J. Kavitha, S.W. Li, C.S. Hsu, Y. Chi, Y.S. Yeh, Platinum(II) complexes with pyridyl azolate-based chelates: synthesis, structural characterization, and tuning of photo- and electrophosphorescence, Inorg. Chem. 45 (2006) 137–146.
[51] S.Y. Chang, J. Kavitha, J.Y. Hung, Y. Chi, Y.M. Cheng, E.Y. Li, Luminescent platinum(II) complexes containing isoquinolinyl indazolate ligands: synthetic reaction pathway and photophysical properties, Inorg. Chem. 46 (2007) 7064–7074.
[52] L.K. Tuong, R.W. Chen-Cheng, H.W. Lin, Y.J. Shiau, S.H. Liu, P.T. Chou, Near-infrared organic light-emitting diodes with very high external quantum efficiency and radiance, Nat. Photon. 11 (2016) 63–68.
[53] N. Su, G.Z. Lu, Y.X. Zheng, Highly efficient green electroluminescence of iridium(III) complexes based on (1H-pyrazol-5-yl)pyridine derivatives ancillary ligands with low efficiency roll-off, J. Mater. Chem. C. 6 (2018) 5778–5784.
[54] N. Su, Z.G. Wu, Y.X. Zheng, High efficient bluish green organic light-emitting diodes of iridium(III) complexes with low efficiency roll-off, Dalton Trans. 47 (2018) 7587–7593.
[55] V. Montoya, J. Pons, X. Solans, M. Font-Bardia, J. Ros, Synthesis and characterisation of new N1-alkyl-3,5-dipyridylpyrazole derived ligands. Study of their reactivity with Pd(II) and Pt(II), Inorg. Chim. Acta. 358 (2005) 2763–2769.
[56] Y.M. Jin, C.C. Wang, L.S. Xue, T.Y. Li, S. Zhang, X. Liu, Efficient organic light-emitting diodes with low efficiency roll-off using iridium emitter with 2-(5-phenyl-1,3,4-oxadiazol-2-yl)phenol as ancillary ligand, J. Organomet. Chem. 765 (2014) 39–45.
[57] Q.L. Xu, C.C. Wang, T.Y. Li, M.Y. Teng, S. Zhang, Y.M. Jing, Syntheses, photoluminescence, and electroluminescence of a series of iridium complexes with trifluoromethyl-substituted 2-phenylpyridine as the main ligands and tetraphenylimidodiphosphinate as the ancillary ligand, Inorg. Chem. 52 (2013) 4916–4925.
[58] H. Cao, H. Sun, Y. Yin, X. Wen, G. Shan, Z. Su, Iridium(III) complexes adopting 1,2-diphenyl-1H-benzoimidazole ligands for highly efficient organic light-emitting diodes with low efficiency roll-off and non-doped feature, J. Mater. Chem. C. 2 (2014) 2150.
[59] C.H. Yang, Y.M. Cheng, Y. Chi, C.J. Hsu, F.C. Fang, K.T. Wong, Blue-emitting heteroleptic iridium(III) complexes suitable for high-efficiency phosphorescent OLEDs, Angew. Chem. Int. Ed. 46 (2007) 2418–2421.
[60] Z.J. Xu, R. Fang, C. Zhao, J.S. Huang, G.Y. Li, N. Zhu, Cis-Beta-bis(carbonyl) ruthenium-salen complexes: X-ray crystal structures and remarkable catalytic properties toward asymmetric intramolecular alkene cyclopropanation, J. Am. Chem. Soc. 131 (2009) 4405–4417.
[61] E. Orselli, G.S. Kottas, A.E. Konradsson, P. Coppo, R. Frohlich, L.D. Cola, Blue-emitting iridium complexes with substituted 1,2,4-triazole ligands: synthesis, photophysics, and devices, Inorg. Chem. 46 (2007) 11082–11093.
[62] C.H. Yang, K.H. Fang, W.L. Su, S.P. Wang, S.K. Su, I.W. Sun, Color tuning of iridium complexes for organic light-emitting diodes: the electronegative effect and π-conjugation effect, J. Organomet. Chem. 691 (2006) 2767–2773.
[63] H.Y. Li, L. Zhou, M.Y. Teng, Q.L. Xu, C. Lin, Y.X. Zheng, Highly efficient green phosphorescent OLEDs based on a novel iridium complex, J. Mater. Chem. C 1 (2013) 560–565.
[64] Y.H. Zhou, J. Xu, Z.G. Wu, Y.X. Zheng, Synthesis, photoluminescence and electroluminescence of one iridium complex with 2-(2,4-difluorophenyl)-4-(trifluoromethyl)pyrimidine and tetraphenylimidodiphosphinate ligands, J. Organomet. Chem. 848 (2017) 226–231.
[65] J.C. Xia, X. Liang, Z.P. Yan, Z.G. Wu, Y. Zhao, Y.X. Zheng, W.W. Zhang, Iridium(III) phosphors with bis(diphenylphorothioyl)amide ligand for efficient green and sky-blue OLEDs with EQE nearly 28%, J. Mater. Chem. C 6 (2018) 9010–9016.